ISSN 2411-3336; e-ISSN 2541-9404

JOURNAL OF MINING INSTITUTE

Zapiski Gornogo instituta

Journal homepage: pmi.spmi.ru

Research article
UDC 551.71:552.4 (470.22)

The problem of the genesis of the Mesoarchean aluminosilicate rocks from the Karelian craton and their possible use as a quartz-feldspar raw material

Natalya I. KONDRASHOVA[1,2], **Tatyana P. BUBNOVA**[1], **Pavel V. MEDVEDEV**[1]✉
[1] *Institute of Geology, Karelian Research Centre of the RAS, Petrozavodsk, Russia*
[2] *Petrozavodsk State University, Petrozavodsk, Russia*

How to cite this article: Kondrashova N.I., Bubnova T.P., Medvedev P.V. The problem of the genesis of the Mesoarchean aluminosilicate rocks of the Karelian craton and their possible use as a quartz-feldspar raw material. Journal of Mining Institute. 2022. Vol. 257, p. 720-731. DOI: 10.31897/PMI.2022.65

Abstract. The article presents original data obtained in the study of the chemical and mineral compositions of the Late Archean aluminosilicate rocks (formerly called silicites) from the Koikari and Elmus structures of the Vedlozero-Segozero greenstone belt of the Karelian craton (Central Karelia). A comprehensive study of these formations revealed their complex genesis as a result of the late imposition of hydrothermal and metamorphic alteration on sedimentary and volcanic-sedimentary rocks of feldspar-quartz composition. Due to the superimposed metasomatic (temperature?) impact on feldspar-quartz siltstones, Fe was removed from microinclusions in quartz and feldspar and its oxides were concentrated along the grain boundaries. Minerals such as monazite, parisite, allanite are also located either along the grain boundaries of quartz and feldspars, or together with calcite they fill microfractures, which makes it possible to get rid of them when preparing quartz-feldspar concentrates using various beneficiation technologies. According to most indicators limited by GOSTs, individual samples in their natural form meet the requirements for quartz-feldspar raw materials for use as part of batch in the production of diverse types of glass. Additional beneficiation of the feedstock (grinding, screening into narrow classes and further magnetic separation) leads to a decrease in Fe_2O_3 content to normalized values. The resulting quartz-feldspar concentrates with various particle sizes can be used in the production of building material and fine ceramics (sanitary and ceramic products, facing and finishing tiles, artistic, household porcelain and faience). The homogeneity of the mineral and chemical composition, the possibility of compact extraction and beneficiation (including in mobile small-sized installations) increase the prospects and competitiveness of this non-traditional feldspar raw material from Central Karelia.

***Keywords*:** feldspar-quartz; aluminosilicate rocks; quartz-feldspar concentrate; Elmus and Koikari structures; Vedlozero-Segozero greenstone belt; Karelian craton

Acknowledgment. The studies were carried out under the state task of the Institute of Geology, Karelian Research Centre of the RAS (AAAA-A18-118020290085-4 and AAAA-A18-118020290175-2).

***Received*: 22.02.2022** ***Accepted*: 15.09.2022** ***Online*: 19.10.2022** ***Published*: 10.11.2022**

Introduction. Currently, there is a growing interest in the search for new sources of raw materials for the industry of the Russian Federation [1-3]. As an example of an alternative source for obtaining quartz-feldspar concentrates, volcanogenic sedimentary and volcanogenic chemogenic formations of the Late Archean greenstone belts of Karelia are proposed [4-6]. The authors of [7, 8] recognize their hydrothermal metasomatic genesis, believing that the formation of these rocks, the mineral composition of which is dominated by quartz and feldspars, was confined to the activity of underwater hydrothermal systems that existed in the areas of the Mesoarchean active volcanism. In [3, 4, 9], their hydrothermal genesis is not questioned. The authors of studies [10, 11], recognizing the hydrothermal sedimentary genesis of silicites, believe that the latter were formed in back-arc basins during the chemical precipitation of silica from colloidal solutions supplied by underwater hydrothermal systems.

DOI: 10.31897/PMI.2022.65

Journal of Mining Institute. 2022. Vol. 257. P. 720-731

Considering that the places of possible hydrothermal discharge at geochemical barriers are of interest in metallogenic zoning, the petrogeochemical characteristics of rocks positioned as silicites from two local structures of the Vedlozero-Segozero greenstone belt were studied. The purpose of the work was to clarify the genesis of these formations, as well as to establish their geochemical trend in order to assess their possible use as a source of aluminosilicate raw materials.

In the works of the IG KarRC RAS [4-6, 8] the term "silicites" is used as an identical one to describe rocks consisting of quartz and feldspars and containing 71-77 % SiO_2 and 13-16 % Al_2O_3. According to the definition given in the Geological Dictionary (Geological Dictionary. 2011. Vol. 2), "silicite is a rock composed of very fine mineral aggregates of free or aqueous silica ...". The rocks that will be discussed below cannot be attributed to silicites. Given the incorrect identification of the described rocks with silicites, based on their chemical composition, the authors of the article use the term "aluminosilicate or high-silica/siliceous rock" for their designation, or, given the predominance of quartz and feldspar in their mineral composition, "feldspar-quartz rock".

Geological characteristic. The Meso- and Neo-Archean greenstone belts formed on the Paleo-archean granitoid basement, occupy about 20 % of the Karelian craton (Fig.1). At the level of the modern erosion truncation, they are represented by local structures, with the horizons of high-silica rocks present in most of the sections [12].

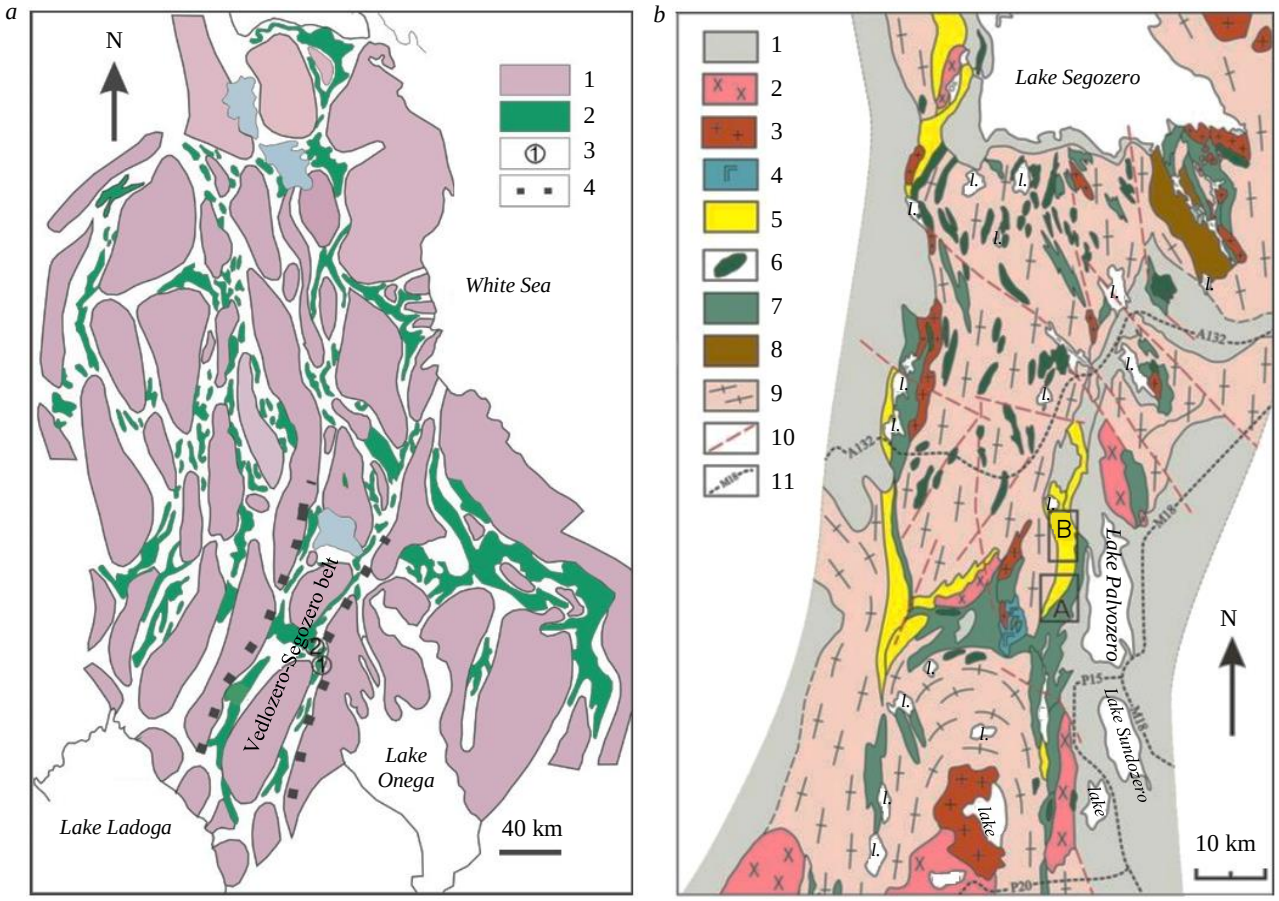

Fig.1. Scheme of the Archean greenstone belts of the Karelian craton (*a*), geological structure of the central part of the Vedlozero-Segozero greenstone belt (*b*) [4, 7, 12]

a: 1 – basement blocks; 2 – greenstone belts; 3 – local structures: Koikari (1), Elmus (2); 4 – boundaries of the Vedlozero-Segozero greenstone belt; *b*: Koikari (A), Elmus (B) structures. Paleoproterozoic: 1 – supracrustal complexes; Archean: 2 – diorites, granodiorites, sanukitoids aged at 2.74 Ga years; 3 – granites; 4 – gabbro-diorites; 5 – andesite-rhyolitic association with intraformational sedimentary rocks (tuffs, aluminosilicate rocks, sandstones, dolomites); 6 – amphibolites, gabbroids; 7 – komatiite-basalt associations and intraformational sedimentary rocks; 8 – basalt-dacite andesite association with intraformational sedimentary rocks (tuffs, tuffites, siltstones); 9 – gneiss-granites and migmatite-granites; 10 – large faults; 11 – car roads

Journal of Mining Institute. 2022. Vol. 257. P. 720-731 DOI: 10.31897/PMI.2022.65

The Vedlozero-Segozero belt, stretching in the near-meridional direction from Lake Vedlozero to Lake Segozero in Central Karelia consists of a number of separate structures (Fig.1, *a*), including Elmus and Koikari (Fig.1) [4, 13].

In the Koikari structure, aluminosilicate rocks occur at two levels. In the lower part of the section, they are part of the komatiite-basalt association, occurring among thinly bedded komatiite tuffs. Their formation is associated with gas-hydrothermal activity, which caused a high degree of hydrothermal processing of individual parts of lava flows and the simultaneous influx of silica into the basin [4]. The aluminosilicate rocks studied by us belong to the overlying dacite-rhyolite association (Fig.2). They are confined to the volcanic-terrigenous sequence, consisting of tuff sandstones, greywackes, quartz sandstones, dacite tuffs, pyrite ores, carbonate rocks, and graphitic shales. This sequence replaces intermediate and felsic volcanic rocks both upsection and laterally. Aluminosilicate rocks are to 60 m thick. The section ends with a sequence of quartz-sericite schists. Aluminosilicate rocks of this level in the section are traditionally classified as chemogenic-pyroclastic deposits. Their formation is associated with fumarolic activity, which caused the influx of silica and aluminium into the basin after the weakening of volcanic explosions [4].

In the Elmus structure section, high-silica rocks are part of the andesite-dacitic, rhyolite associations (Fig.2). They form horizons in the upper parts of the volcanogenic sedimentary section about 100 m thick, represented by alternating polymictic conglomerates, sandstones, dacitic tuffs, and tuffites; feldspar greywackes; dolomites with interlayers of carbonaceous siltstones. Thickness of siliceous rocks in the section ranges from 1-2 to 30-50 m, while their massive varieties form layers to 30 m thick sustained along the strike.

The age of host rocks in both structures corresponds to the interval of 3.0-2.84 Ga [7, 8]. The rocks were metamorphosed under conditions of chlorite-sericite subfacies of greenschist facies of regional metamorphism [14].

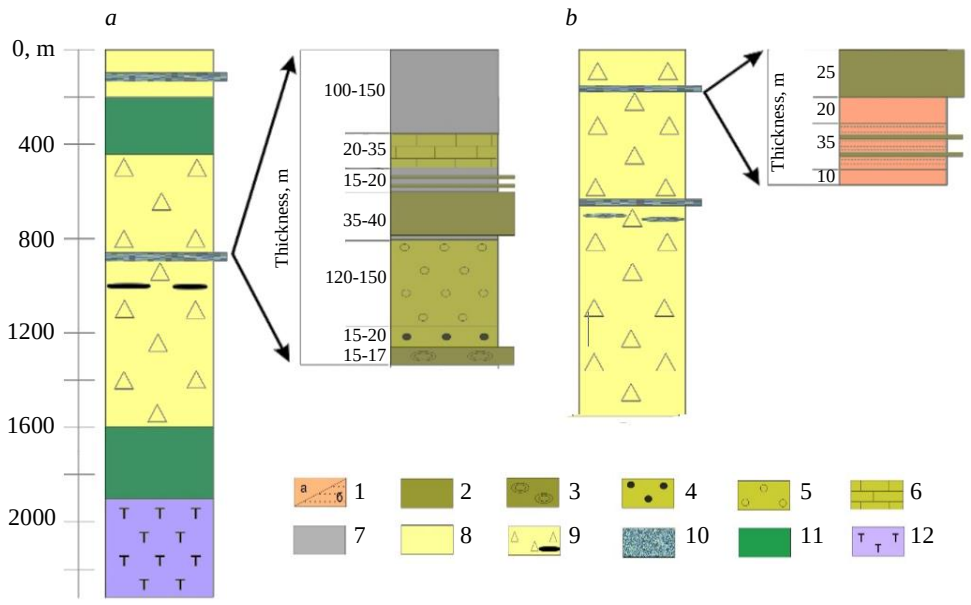

Fig.2. Aluminosilicate rocks in sections of the Koikari (*a*) and Elmus (*b*) structures in the Vedlozero-Segozero greenstone belt of the Karelian craton

1 – massive red aluminosilicate rocks (a), layered pink aluminosilicate rocks with interlayers of gray varieties (b); 2 – massive gray siliceous rocks; 3 – chemogenic concretional silicites; 4 – polymictic conglomerates; 5 – greywackes; 6 – carbonate rocks; 7 – carbonaceous shales; 8 – quartz-sericite schists; 9 – lavas, lava breccias, andesidacite tuffs, dacite tuffites, polymictic conglomerates, sandstones, greywackes, dolomites, interlayers of carbonaceous siltstones and sulphur-pyrite ores; 10 – quartz-feldspar siltstones, siliceous tuffites, chemogenic quartzites; 11 – pillow and massive basalts; 12 – komatiite basalts, komatiites, tuff-tuffites of mafic and komatiite compositions

DOI: 10.31897/PMI.2022.65

Journal of Mining Institute. 2022. Vol. 257. P. 720-731

Methodology. Samples of aluminosilicate rocks were taken from sections in the Koikari and Elmus structures of the Vedlozero-Segozero greenstone belt. We studied laboratory samples weighing 5 kg each, taken from three outcrops in each structure: 6 samples from the Koikari and 12 samples from the Elmus structures. 18 thin sections and 10 polished sections were studied. The petrographic description of rocks in thin sections was performed using an optical microscope POLAM R-211 (O.V.Bukchina). All analytical work was carried out on the equipment complex at the Centre for Collective Use of the Federal Research Centre "Karelian Research Centre of the Russian Academy of Sciences". The content of petrogenic elements and semi-quantitative determination of microadmixtures were identified on an X-ray fluorescence spectrometer Thermo Scientific ARL Advant'X (S.V.Burdyukh) according to the standard procedure. The determination accuracy was 0.0005 % for MnO, 0.0034 % for TiO_2, 0.025-0.035 % for magnesium and calcium oxides, 0.10-0.11 % for Na_2O-K_2O. The error in determining the concentration of Al_2O_3 is 0.17 % and for SiO_2 is 0.22 %. Chemical composition of the samples was studied using an X-SERIES 2 Terhmo quadrupole mass spectrometer (A.S. Paramonov). Limits of detection are, mg/kg (ppm): Pr, Sm-Lu, U – 0.03, Nb, Nd, Cs – 0.04, Y, Hf, La – 0.05, Ce, Pb, Th, Co – 0.06, Mo – 0.12, Zr – 0.81, Li – 0.30, Rb – 0.52, Sr, Ni, Cu – 1.01-1.44, Mn – 2.26, Sc – 2.61, V and Cr – 5.94-5.96, Ba – 24.12 and Zn – 25.06. The morphology and features of the chemical composition of minerals were determined using a scanning electron microscope (SEM) VEGA II LSH (Tescan) with an energy dispersive microanalyzer INCA Energy 350 (Oxford instruments).

Mineralogical and petrographic characteristics. The investigated rocks in both structures are characterized by a thin-bedded texture (Fig.3, *a*, *b*). The sections also contain massive varieties with elements of lenticular-banded and brecciated textures (Fig.3, *c*-*f*).

In the Koikari structure, the mineral composition of the studied rocks includes quartz (20-42 %), sericite (to 15 %) and feldspars (20-34 %), sometimes there are fragments of potassium feldspar (K-feldspar), plagioclase, flakes of biotite, muscovite, and lamellar and fine-flake chlorite. The rocks are fine-grained, often composed of alternating light and dark bands of different mineral composition. The predominant mineral in the light part of the rock is quartz with clear even boundaries and grain sizes from 0.005×0.01 to 0.05×0.07 mm; 0.04×0.11 mm, with smooth extinction.

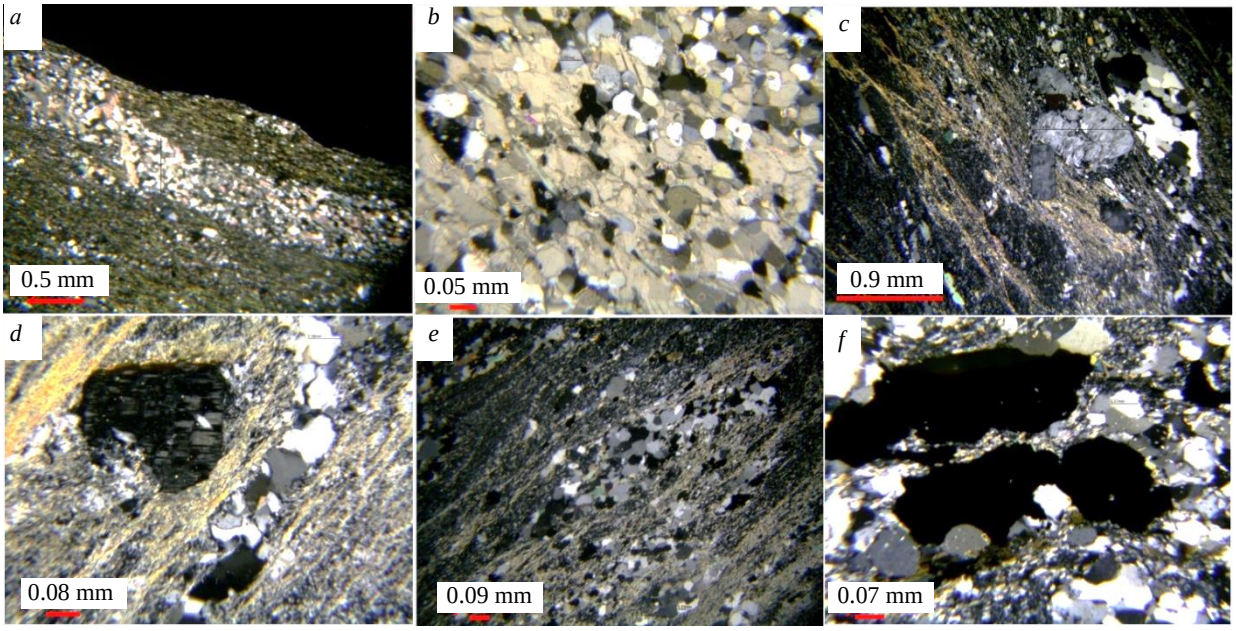

Fig.3. Aluminosilicate rocks of the Koikari and Elmus structures. Optical microscope, polarized light Koikari structure:
a – general view of the rock; *b* – light "bands" composed of quartz, feldspar, calcite;
c – brecciated siliceous rock with K-feldspar fragments;
Elmus structure: *d* – fine-grained rock of quartz-microcline-sericite composition with a feldspar fragment;
e – lenticular-banded texture; *f* – iron oxides (dark) in a quartz-feldspar matrix

Journal of Mining Institute. 2022. Vol. 257. P. 720-731 DOI: 10.31897/PMI.2022.65

The dark bands are dominated by sericite, chlorite, and fine grains of quartz elongated along schistosity. The structure of the rocks is silty, silty-psammitic, in some places granoblastic, lepidogranoblastic, which enables to attribute them to metamorphosed siltstones, partly to silty sandstones (Fig.3, *a*, *b*, *f*).

The brecciated varieties contain fragments of K-feldspar, rounded segregations of recrystallized quartz, fragments of siliceous concretions, which are cemented by a finely crystalline aggregate consisting of quartz, sericite, and calcite. The general appearance of massive aluminosilicate rocks is due to a thin intergrowth of albite, quartz, and microcline (Fig.4, *a*-*c*). Muscovite, rutile, calcite, monazite, allanite, parasite, and zircon are found along the grain boundaries of quartz and microcline, quartz, and albite, in microfractures of these minerals (Fig.4, *d*-*f*).

The main rock-forming minerals for the studied rocks in the Elmus structure are quartz (29-49 %), microcline (8-14 %), and albite (9-45 %), with a grain size of 0.1 to 0.01 mm. Rock structure is blastosiltstone, which makes it possible to classify them as metasiltstones. There are areas with a psammite structure, which does not exclude the presence of silty sandstone inclusions among the aluminosilicate rocks. Muscovite, the content of which varies from 1-2 to 14 %, as a rule, is represented by thin flakes 0.02-0.01 mm, parallel to the general schistosity of the rock (Fig.5, *a*-*c*). Quartz of two generations is present. Fine-grained quartz with diffuse outlines, developed in close intergrowth with feldspars, predominates (Fig.5, *b*). Quartz of the second generation is represented by recrystallized large grains of distinct shapes with sizes to 0.18×0.14 mm and forms veinlets and lenticular nests oriented parallel to the rock schistosity. The shape of individual microcline grains indicates their development over felsic ash material (Fig.5, *c*).

Biotite and rare grains of apatite, stilpnomelane, magnetite, ilmenite, and zircon occur in the form of single black-brown and greenish-brown plates. Biotite is partially replaced by thin-lamellar light green chlorite. Rare-earth mineralization associated with small, scattered grains of allanite, parisite, monazite, located along the grain boundaries of quartz, microcline, and albite, or occurring

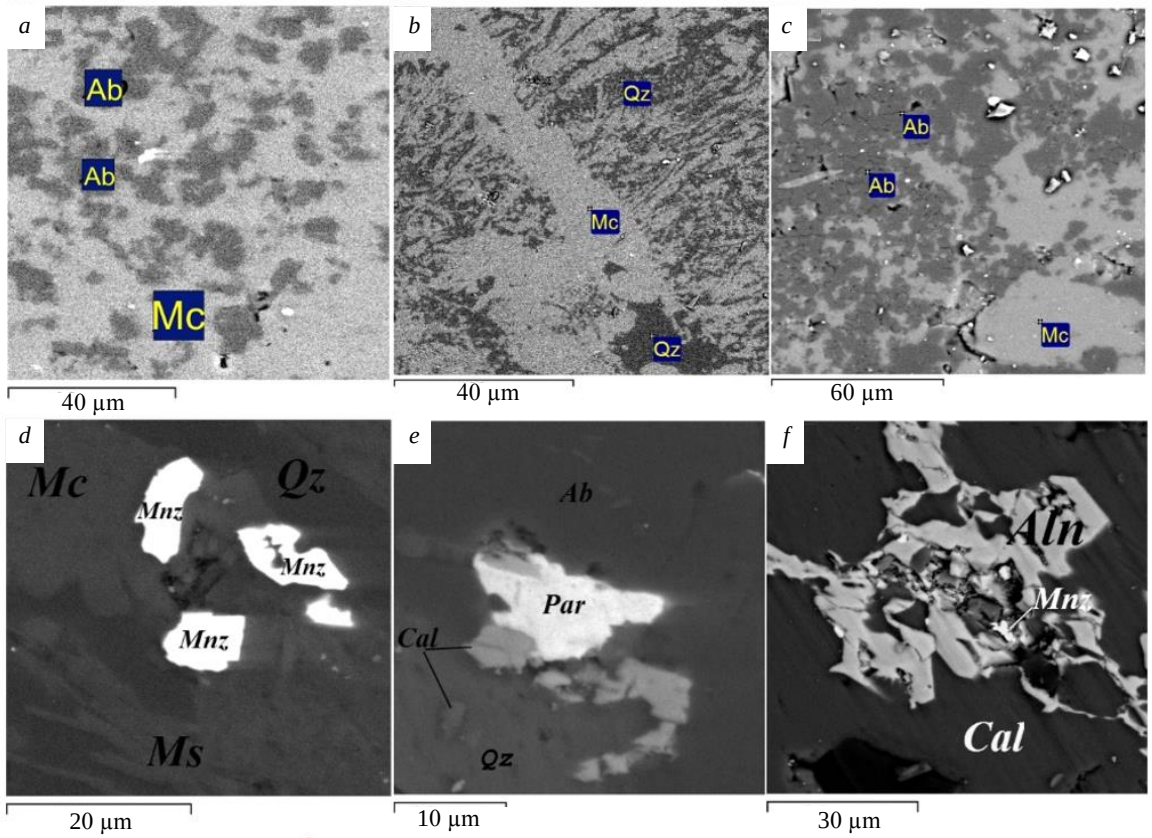

Fig.4. Aluminosilicate rocks of the Koikari structure. SEM VEGA II LSH image, BSE detector

Qz – quartz, Mc – microcline, Ab – albite, Ms – muscovite, Cal – calcite, Mnz – monazite, Par – parisite, Aln – allanite

DOI: 10.31897/PMI.2022.65

Journal of Mining Institute. 2022. Vol. 257. P. 720-731

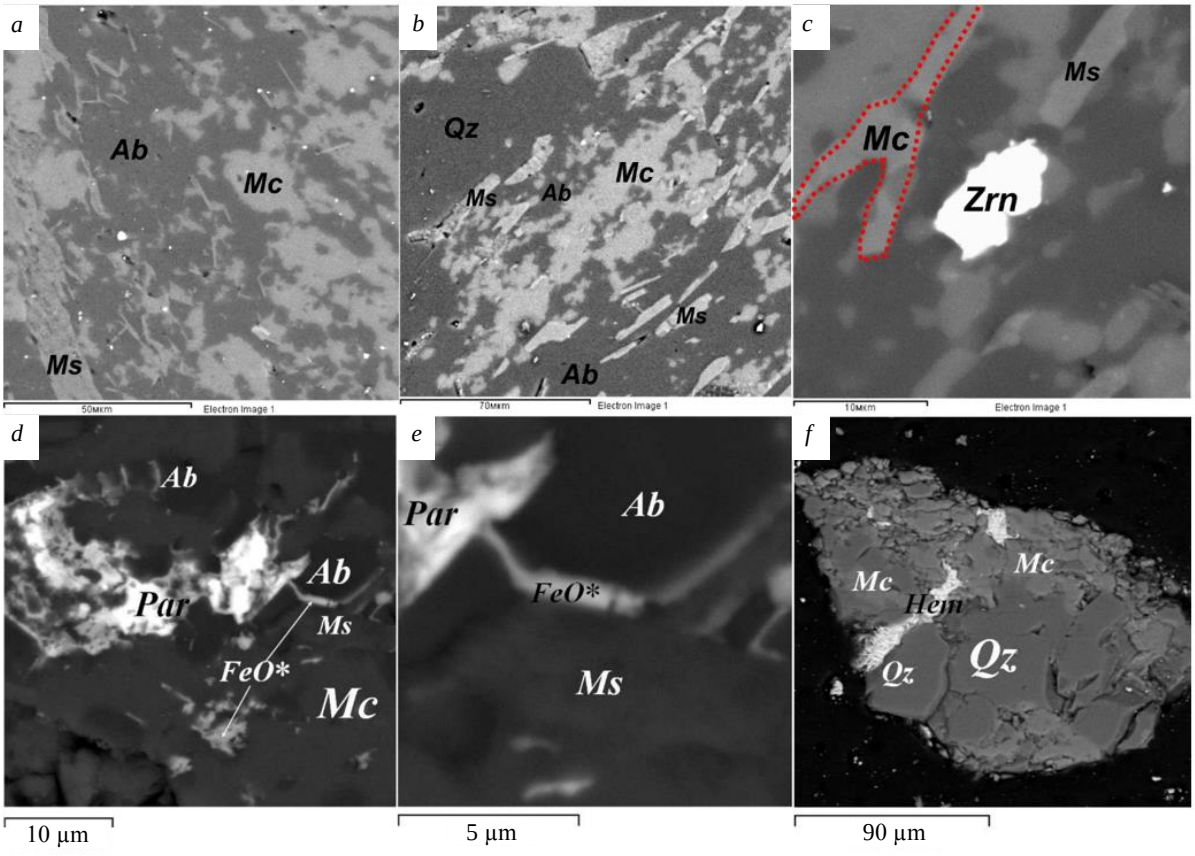

Fig.5. Textural and structural features of aluminosilicate rocks of the Elmus structure (*a*-*e*), quartz-feldspar concentrate (*f*). SEM VEGA II LSH image, BSE detector

Zrn – zircon, Hem – hematite, FeO* – iron oxides of unclear mineral composition

together with calcite in microfractures was found in the aluminosilicate rocks of the Elmus structure (Fig.5, *d*-*f*).

In the aluminosilicate rocks of both structures, grains of quartz and feldspars are noted, filled with tiny flakes of sericite and chains of gas-liquid inclusions, which record microfractures. In some microfractures, there is a finely dispersed, undetectable ore substance of a ferruginous composition.

The possible formation of part of the studied rocks over dacite lavas is not ruled out. Structure sections contain dacites with quartz amygdales, plagioclase phenocrysts (15-30 % An), and groundmass composed of quartz and feldspar crystals [4]. Among the aluminosilicate rocks of the Koikari structure, there are interbeds with similar amygdales (?) of quartz, which we identified as altered felsic lavas.

Mineral composition of the high-silica rocks in both structures contains secondary calcite and epidote, and later microveinlets of quartz composition are noted.

Petrogeochemical composition. The differing mineral composition determines the differences in the chemical composition of the studied rocks in both structures, primarily in the content of alumina, oxides of titanium, iron, magnesium, and sodium (see Table).

Silica content is quite variable both for aluminosilicate rocks of the Elmus (71.14-79.59 %) and formations of the Koikari structure (52.79-75.21 %). Significant fluctuations are also noted in the concentrations of other oxides. Such scattered values of petrogenic components do not contradict the conclusion that these formations are classified as siltstones and do not confirm the assumption about the predominant supply of silica with hydrothermal fluids during the formation of the studied aluminosilicate rocks [11]. With the prevailing supply of silica by hydrothermal fluids, the beneficiation of the formed rocks in Fe, Mn [15], Mo should be observed, which in reality does not occur. It was

shown [16] that the mechanism and rate of precipitation of hydrothermal silica is controlled by the rate of formation of Fe hydroxides, since iron not only precipitates silica, but also protects it from subsequent dissolution.

Chemical (wt.%) and trace element (mg/kg or ppm) composition of aluminosilicate rocks from the Elmus and Koikari structures

Oxide (element)	Koikari structure						Elmus structure											
	Sample numbers																	
	K1-1	K1-2	K2-1	K2-2	K3-1	K3-2	E-4-1	E-4-2	E-4-3	E-4-4	E-5-1	E-5-2	E-5-3	E-5-4	E-6-1	E-6-2	E-6-3	E-6-4
SiO_2	70.24	75.21	74.42	59.58	52.79	70.71	75.5	73.76	73.94	75.21	79.59	76.81	75.87	75.51	74.35	75.11	74.07	71.14
TiO_2	0.099	0.082	0.07	0.89	0.91	0.1	0.07	0.07	0.07	0.09	0.06	0.07	0.06	0.07	0.08	0.08	0.08	0.06
Al_2O_3	13.89	13.28	13.81	22.41	19.75	12.96	13.15	13.48	13.53	12.38	11.02	11.82	13.26	12.06	13.9	13.64	14.3	11.68
Fe_2O_3	1.42	0.853	0.87	2.81	6.86	1.51	0.69	1.12	1.26	0.69	0.87	0.42	0.66	1.41	1.18	1.08	0.93	1.07
CaO	0.35	0.09	0.98	0.12	3.58	4.47	0.71	1.01	1.02	0.96	0.45	0.25	0.33	0.75	0.95	6.4	0.09	6.71
MgO	5.44	2.03	2	5.12	10.48	3.66	0.51	0.87	0.67	1.04	1.56	0.78	0.59	1.23	1.06	13.64	0.55	1.86
Na_2O	0.96	1.16	1.91	0	1.73	1.48	4.79	3.97	3.27	1.07	1.84	1.47	5.2	4.26	2.83	2.58	3.19	4.22
K_2O	7.26	7.06	5.68	8.66	3.08	4.69	4.29	5.38	5.9	8.22	4.3	8.07	3.83	4.29	5.34	6.4	6.53	2.94
Li	11	7.699	16.76	65.25	53.55	21.21	6.256	11.82	18.88	7.098	14.03	3.722	5.809	7.152	14.33	13.28	11.26	4.304
P	207.9	152.3	191.2	240.9	1184	228	165.8	178	173.5	163.8	155.4	159.9	172.5	193.2	145.5	172.5	155.8	158.4
Sc	7.474	5.053	5.217	20.55	24.28	6.854	4.101	6.573	10.64	4.944	1.737	2.6	2.804	2.997	3.472	7.25	3.445	2.712
V	0.863	<PO	<PO	89.09	120.5	7.305	<PO	<PO	<PO	<PO	<PO	<PO	<PO	<PO	<PO	<PO	<PO	<PO
Cr	221.2	17.49	16.49	164.3	303.6	54.54	28.08	23.22	20.56	66.86	32.06	18.41	37.48	48.95	44.27	120.2	66.74	56.55
Mn	148.6	34.96	403.5	132.5	1690	1342	66.08	250.3	150.4	84.79	116.6	40.57	52.04	117	213.9	259.8	93.87	553.2
Co	8.38	0.481	1.3	3.406	26.41	4.071	<PO	<PO	<PO	1.275	0.479	0.761	<PO	1.823	0.392	4.634	2.131	1.909
Ni	129.7	10.23	8.216	36.09	145.3	30.82	5.684	8.487	4.156	11.45	9.932	7.129	7.804	25.13	10.22	70.96	34.88	27.58
Cu	12.82	8.037	5.075	9.442	12.69	8.093	6.054	5.878	3.987	8.647	4.976	10.08	5.429	14.8	5.046	7.43	10.28	7.907
Zn	20.69	21.45	40	40.83	310.6	62.26	26.79	78.03	165.4	21.74	22.49	12.42	188.2	992.4	52.73	69.33	48.78	355.1
As	<PO	<PO	<PO	<PO	27.82	<PO	<PO	<PO	<PO	<PO	<PO	<PO	<PO	<PO	<PO	<PO	<PO	<PO
Rb	142.4	125.6	116.5	283.2	69.7	103.9	104.9	136.9	170.3	119.2	84.41	106	86.17	95.57	138.5	134.3	136.1	63.47
Sr	28.69	22.62	43.5	9.672	61.37	80.79	38.04	35.04	32.86	28.55	21.84	29.62	37.81	42.67	45.62	39.39	40.97	113.6
Y	18.25	13.99	20.86	77.5	17.33	24.8	27.45	28.84	33.94	15.54	13.65	12.22	27.48	33.15	24.3	25.22	15.94	23.14
Zr	32.35	25.08	25.15	52.99	38.38	25.01	24.97	24.82	25.16	25.44	19.23	23.87	22.31	21.41	26.16	23.91	23.31	18.61
Nb	13.33	10.91	9.978	21.08	7.235	8.919	12.19	11.79	10.17	10.24	7.279	8.918	11.14	11.99	12.55	12.17	12.47	9.75
Mo	0.357	0.464	0.476	0.364	0.38	1.355	0.23	0.44	0.47	0.79	0.3	0.61	0.39	0.37	0.21	0.34	0.17	0.239
Cs	4.28	3.34	3.78	7.61	2.98	3.77	1.87	1.83	2.17	2.91	2.30	2.25	2.34	2.76	1.32	1.3	1.26	0.58
Ba	1719	1385	1506	1805	936.60	1163	846.20	1036	1207	1490	981.70	1387	629.30	697.10	869.20	829.90	796	381.70
La	21.64	20.32	38.84	83.04	29.68	37.13	64.73	21.83	21.50	36.93	33.67	27.52	22.42	45.31	13.18	24.11	15.48	42.71
Ce	38.09	34.39	62.35	130.60	42.68	60.12	108.98	39.75	34.22	58.44	51.78	43.42	38.92	75.43	16.44	25.53	28.24	60.97
Pr	6.49	5.95	10.34	22.38	6.79	10.38	18.81	7.09	6.36	10.13	8.44	7.34	6.65	11.90	3.27	5.46	4.07	11.29
Nd	22.33	20.08	35.45	76.40	22.88	35.00	67.01	26.24	23.26	33.23	29.04	23.97	23.78	43.68	11.49	20.15	14.12	39.92
Sm	6.09	5.24	8.74	18.67	5.24	8.64	16.45	7.98	7.10	7.63	6.81	5.58	6.35	10.80	4.09	5.61	3.60	10.17
Eu	0.71	0.64	0.91	1.51	1.23	0.77	0.89	0.49	0.51	0.70	0.62	0.59	0.46	0.64	0.35	0.45	0.30	0.70
Gd	5.82	4.95	7.88	18.12	5.25	8.01	14.59	8.50	7.92	6.52	6.20	4.97	6.49	10.36	5.07	6.49	3.72	9.11
Tb	0.89	0.65	1.03	2.43	0.72	1.14	1.85	1.27	1.23	0.84	0.70	0.68	1.02	1.35	0.86	1.02	0.56	1.16
Dy	4.72	3.63	5.09	14.02	3.95	5.72	8.51	7.19	7.35	4.20	3.26	3.78	5.87	7.45	5.30	5.61	3.57	5.77
Ho	0.91	0.68	0.95	2.77	0.78	1.06	1.33	1.35	1.46	0.75	0.57	0.65	1.14	1.40	1.02	1.06	0.71	1.02
Er	2.89	2.09	2.85	8.71	2.40	3.22	3.55	3.94	4.25	2.22	1.79	1.92	3.49	4.11	3.02	3.01	2.26	3.04
Tm	0.42	0.32	0.42	1.35	0.35	0.47	0.50	0.56	0.59	0.31	0.26	0.29	0.52	0.60	0.43	0.42	0.31	0.43
Yb	3.10	2.44	3.01	9.04	2.52	3.53	3.63	3.99	4.12	2.36	2.02	2.01	3.78	4.26	2.94	2.80	2.40	3.25
Lu	0.45	0.35	0.44	1.39	0.37	0.51	0.55	0.56	0.60	0.35	0.29	0.29	0.54	0.61	0.43	0.40	0.35	0.45
Hf	5.66	4.51	4.29	6.34	4.43	4.28	4.74	4.85	4.98	4.28	3.20	3.86	4.10	3.94	4.82	4.30	4.34	3.66
Pb	5.13	4.03	7.59	5.41	56.09	14.95	20.82	14.97	35.44	8.10	3.42	4.89	9.55	10.66	4.45	4.86	4.63	6.21
Th	18.45	14.60	14.93	10.54	7.34	16.16	11.95	11.71	11.40	15.42	11.22	13.28	9.69	11.07	13.20	13.80	10.34	12.62
U	3.12	2.50	4.63	11.56	1.47	4.92	2.56	3.15	2.96	3.52	2.13	3.01	2.50	2.61	2.59	3.23	2.44	2.24

Note. < PO – below the detection limits.

During the petrographic study of high-silica rocks, traces of ash particles of felsic composition were found. The lithochemical data confirm both the presence of felsic pyroclastic rocks and do not exclude mafic pyroclastic rocks.

The investigated rocks from both structures are characterized by an anomalously low value of the titanium modulus (TM), TiO_2/Al_2O_3, the range of changes of which is 0.005-0.008. Such TM values can be associated with the presence of felsic pyroclastic rocks in them. For two samples from the Koikari structure, the TM values are 0.04 and 0.046. Such values are characteristic of deep-water sedimentary deposits [17]. In addition, for aluminosilicate rocks of this structure, a positive correlation of TiO_2-Al_2O_3 with a reliability of 0.94 was noted, which is also characteristic along with a negative TiO_2-SiO_2 correlation (certainty factor 0.91) of sedimentary formations.

DOI: 10.31897/PMI.2022.65

Journal of Mining Institute. 2022. Vol. 257. P. 720-731

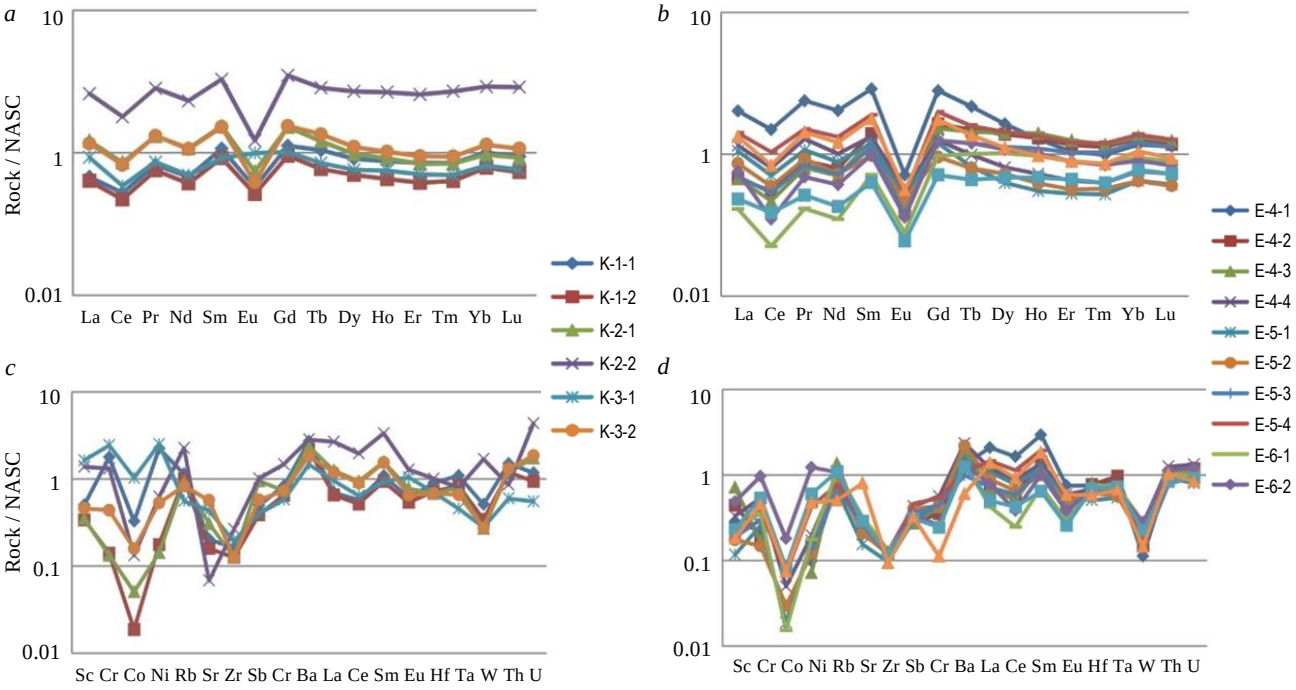

Fig.6. REE distribution spectra in aluminosilicate rocks of the Koikari (*a*) and Elmus (*b*) structures and spider diagrams of the distribution of trace elements in the same rocks of the Koikari (*c*) and Elmus (*d*) structures. Normalised to North American Shale (NASC) [19]

The anomalously high values of the hydrolysate modulus (HM = Al_2O_3 + TiO_2 + Fe_2O_3 + FeO + + MnO/SiO_2) for some samples from the Koikari structure section (0.44 and 0.53) unambiguously indicate the presence of mafic pyroclastic rocks in their composition, which is also confirmed by the increased content of MgO in these samples [18].

Rare earths. According to the content of rare earth elements (REE), the siliceous rocks from the two regions are almost identical (see Table, Fig.6, *a*, *b*). The total content of lanthanides in the formations of the Elmus structure is 67.86-311.34 g/t, in similar rocks of the Koikari structure it varies from 101.73 to 390.41 g/t. Taking into account that the REE concentration in siliceous formations is insignificant [20, 21], and in clays and shales the total content of lanthanides is about 195.42 ppm, it is possible to associate the observed increased REE values with the presence of pyroclastic rocks, which is also recorded in thin sections and by lithochemical parameters, as well as accessory rare earth minerals along the grain boundaries of quartz, microcline, albite and in microfractures together with calcite.

High-silica rocks of the Koikari structure (Eu/Eu^* = 0.35-0.55) differ from similar formations of the Elmus structure (Eu/Eu^* = 0.25-0.49) by the Eu-anomaly value. The studied formations from the two regions are characterized by a negative Ce-anomaly. For siliceous formations of the Elmus structure, the Ce-anomaly falls within the range of 0.48-0.78; for similar rocks of the Koikari structure, it does not go beyond 0.65-0.70. Positive Eu-, Y-, Ho-anomalies are noted in hydrothermal formations [22, 23]. In the studied formations, the content of holmium is at the level of its concentration in NASC, and yttrium is at the level of post-Archaean shales. Negative Ce-, Eu-anomalies can in this case indicate the interaction of background siliceous deposits of sedimentary genesis with sea water.

If we consider the Ce/La index as a proof of the presence of exhalation material in the formations [24], then for the aluminosilicate rocks from both structures, Ce/La >1. For the formations of the Koikari structure, the value of this indicator falls within the range of 1.44-1.76, and for the rocks of the Elmus structure it varies within 1.06-1.82, which does not confirm the formation of the studied rocks solely due to the active supply of silica by hydrothermal fluids.

The total content of light rare earths (La-Pr) exceeds the content of TREE (Nd-Lu), which also does not allow us to assume a significant contribution of the exhalation component during the formation of the considered rocks. The total content of lanthanides is either less or coincides with their content in NASC shales, except for three samples: 390.4 (K-2-2), 311.34 (E-4-1), and 217.89 ppm (E-5-4), which is due to the presence of accessory minerals and pyroclastic rocks in these samples.

Microelement composition. In the studied rocks from both structures, the contents of Rb, Cs, Hf, Ta, Sb, Th, La-Sm, and U in the formations of the Elmus structure are close to their concentrations in the North American shale. In high-silica rocks of the Koikari structure, decreased concentrations of Co, Ni, Cr, Sr, Zr and increased U are noted (see Table, Fig.6, *c*, *d*). The pattern of spider diagrams for aluminosilicate formations of the Koikari structure differs from that of similar formations of the Elmus structure due to the large intervals of variation in the concentrations of individual elements. In all aluminosilicate rocks from the Koikari structure, an increased content of barium from 936 to 1805 ppm is noted, while its content in the NASC shale is 636 ppm. In some samples, Fe, Mg, Mn, P content is increased.

Discussion. The formation of aluminosilicate rocks can be explained by the supply of silica and alumina by hydrothermal fluids [21, 25, 26] genetically related to volcanic edifices, i.e., recognizing their exclusively hydrothermal metasomatic genesis [27-29]. It is this point of view that was first expressed by A.I.Svetova in 1988 [4] and later duplicated in [3, 6, 7]. However, the petrographic and chemical features of the considered aluminosilicate rocks do not support this point of view. Everything indicates that these formations could have been formed in a sedimentogenic-diagenetic way, without connection with the supply of exhalation material at the time of their formation, which means that there is no genetic connection with volcanoes, confirming only their paragenetic connection. Hydrothermal solutions containing a significant amount of silicic acid have a high adsorption capacity with respect to cations of various metals, especially heavy ones [16, 30]. However, the concentrations of these elements in the formations under consideration are at the level of their content in NASC shales (Fig.6, *c*, *d*). The absence of hydrothermal minerals, which are formed together with silica precipitation, also does not enable to assert an exclusively hydrothermal source of silica and alumina during the formation of the considered aluminosilicate rocks.

In the study of modern long-lived hydrothermal systems [31-33], an increase in Cu, Zn, Cd, Fe, Mn, Mo concentrations and enrichment in rare earths is noted in sediments exposed to hydrothermal fluids. This is not typical of the formations under consideration. The postvolcanic hydrothermal impact was exerted on the original rocks, but due to the absence of faults near or directly in the areas of work, which can be considered fluid conductors, it was not accompanied by a significant supply-subtraction of elements. The impact could be due to an increase in temperature, which, of course, requires additional research.

In the studied rocks, there is a thin intergrowth of feldspars and quartz, areas with a granoblastic structure are present, which is possible both during metasomatism of a quartz-feldspar sedimentary (and/or volcanic, volcanic-sedimentary) rock that already existed in the section, and during regional metamorphism. The aluminosilicate rocks of the Elmus structure contain micas with increased iron content: muscovite with Fe_2O_3 content 4.24-6.8 % and biotite with Fe_2O_3 from 15 to 30 %. Such a high content of iron oxides is usually characteristic of muscovites from shales and biotites from granites that have undergone metamorphic transformations. Volcanic rocks of felsic composition during metamorphism can form muscovite-quartz-feldspar rocks [34].

The authors of [35], having studied the distribution of rare earth and microelements in quartz from the aluminosilicate rocks of the Koikari and Elmus structures, concluded that it had an exclusively sedimentary-chemogenic genesis. There are indications of the possible presence of background siliceous sediments with chemogenic silica deposition in the water basin (Fig.7). Rarely occurring silica globules and filamentous microfossils [11] in thin sections can just be associated with the conditions of siliceous material accumulation in the background regime of a marine basin. This can also be proved by the negative anomalies of cerium and europium, as inherited from sea water, and chlorite

DOI: 10.31897/PMI.2022.65

Journal of Mining Institute. 2022. Vol. 257. P. 720-731

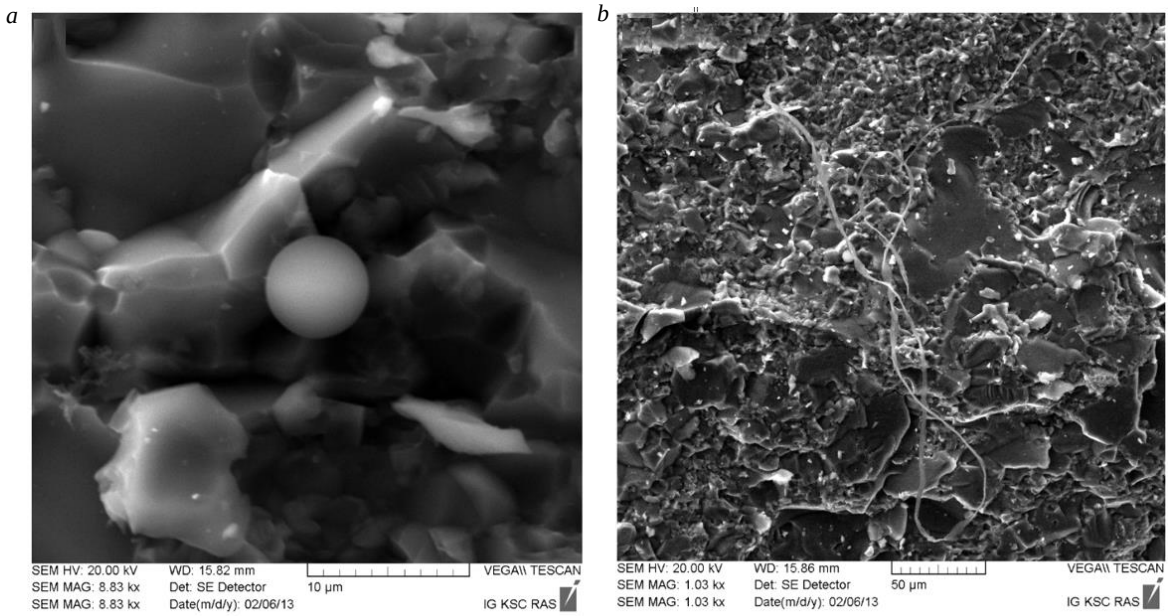

Fig.7. Silica globule (*a*) and filamentous microfossils of Mesoarchean (?) age (*b*)

present in the mineral composition of the studied rocks can be considered as a recrystallized clay substance. The volumes of siliceous chemogenic sediments were insignificant, as evidenced by the absence of a clear vertical stratification of sediments in the section of structures and a significant supply of siliciclastic material.

The observed features of the studied rocks are possibly the result of several processes imposed, which ultimately "purified" aluminosilicate rocks from impurities that are considered harmful in the manufacture of quartz-feldspar concentrates [3, 5, 6]. Due to the superimposed metasomatic (temperature?) impact on quartz-feldspar siltstones, Fe is removed from microinclusions in quartz and feldspar and its oxides are concentrated along the grain boundaries (see Fig.5, *d*, *e*). Minerals such as monazite, parisite, allanite are also located either along the grain boundaries of quartz and feldspars, or together with calcite they fill microfractures (see Fig.4, *d-f*; Fig.5, *d*, *e*), which simplifies their extraction in case of the feedstock beneficiation.

For most of the limited indicators (see Table), individual samples in their natural form meet the requirements for quartz-feldspar raw materials for use in the composition of batches in the production of diverse types of glass (GOST 13451-77: $Fe_2O_3 \leq 0.20$-0.70 % for grade KPShS-N-11.5 not standardized; Al_2O_3 – 11.5-14 %; $K_2O + Na_2O$ – 7-9%; $Si_2O \leq 75$-80 %). In accordance with the requirements for quartz-feldspar raw materials for the production of building materials and fine ceramics, only the content of iron oxide in all samples exceeds the normalized values (GOST 15045-78, GOST 7030-75: $Fe_2O_3 \leq 0.20$-0.30 %). And such indicators as the mass fraction of the sum of calcium and magnesium oxides ($CaO + MgO \leq 1.5$-2.5 %), potassium and sodium ($K_2O + Na_2O$ – 7-9 %), ratio of alkali metal oxides (K_2O/Na_2O – 0.7-0.9 or 2-3 %), mass fraction of quartz (no more than 30-40 %) for most samples are within the acceptable range. Elevated iron contents are associated with the presence of rock-forming muscovite, Fe_2O_3 content in which, according to SEM data, reaches 4.24-6.8, as well as secondary biotite, chlorite, and magnetite. The authors of [3] show that regrinding, screening into narrow classes in accordance with the requirements of GOSTs and further magnetic separation of narrowly classified material lead to a decrease in Fe_2O_3 content (to 0.19 %) and enable to consider the possible use of quartz-feldspar concentrate for sanitary and ceramic products, facing and finishing tiles, artistic, household porcelain and faience. Alternative options for the use of quartz-feldspar rocks from Central Karelia can be the production of high-strength crushed stone, aggregate

of heavy concretes, and filler for various building materials [6]. Their possible use as a raw material for the production of glass-ceramic materials, sitalls, seems to be a promising direction.

Conclusions. The observed chemical characteristics of the studied aluminosilicate rocks arose during the late impact (metasomatosis – metamorphism) on terrigenous sediments with a significant presence of sialic material, and also, possibly, on tuffs and lavas of felsic composition (?). Pyroclastic rocks also contributed to their genesis, recorded both in thin sections and by the values of lithochemical indicators. The subsequent temperature (?) metasomatism, and later regional metamorphism, caused the observed chemical composition of the studied formations and not always unambiguous geochemical characteristics.

The considered rocks were formed as a result of the imposition of several processes, which eventually led to the appearance of aluminosilicate rocks with a minimum content of admixtures that are harmful in the production of quartz-feldspar concentrates. In Russia, the types, parameters, and areas of application of quartz-feldspar and feldspar raw materials in various industries are regulated by GOST 23034-78. The considered aluminosilicate formations in the sections of the Elmus and Koikari structures fully meet the requirements of GOST for the production of porcelain and faience, as well as finishing and facing tiles. The results of studies of aluminosilicate rocks in Central Karelia show their potential use in the natural form and for obtaining quartz-feldspar products for various purposes.

Given the similarity of petrogeochemical composition of the formations under consideration with terrigenous and volcanogenic sedimentary formations from the Paleoproterozoic sections, as well as the paragenetic relationship with volcanic rocks, it is possible to increase the scale of finds of alternative feldspar raw materials. Similar quartz-feldspar formations are also present in other Paleoproterozoic sections of the Karelian craton, where there are no volcanic structures, but a large number of dolerite sills are mapped.

Homogeneous mineral and chemical composition, possible compact extraction and beneficiation (including in mobile small-sized installations) increases the prospects and competitiveness of this non-traditional feldspar raw material. It is possible to find potentially promising targets suitable for obtaining high-quality quartz-feldspar (or quartz) concentrates in Karelia, which in the future will significantly expand the mineral resource base of the Republic of Karelia and North-West Russia.

REFERENCES

1. Berezinskaya O., Vedev A. Dependency of the Russian Industry on Imports and the Strategy of Import Substitution Industrialization. *Voprosy ekonomiki*. 2015. N 1, p. 103-115 (in Russian).

2. Petrov I.M. Critical Minerals in Russia. *Mineral recourses of Russia. Economics and management*. 2016. N 4, p. 27-30 (in Russian).

3. Skamnitskaya L.S., Bubnova T.P., Svetov S.A. Process mineralogy of Karelian high-silica sedimentary rocks – a nonconventional source of quartzfeldspathic mineral material. *Obogashchenie rud*. 2016. N 4, p. 22-28 (in Russian). DOI: 10.17580/or.2016.04.06

4. Svetova A.I. Archean volcanism in the Vedlozero-Segozero greenstone belt of Karelia. Petrozavodsk: Karelskii filial AN SSSR, 1988, p. 147 (in Russian).

5. Svetova E., Bubnova T., Bukchina O. High-Silica Rocks of Central Karelia – A Potential Source of Quartz Raw Material. *Karelian Research Centre of the RAS*. 2020. N 6, p. 106-116 (in Russian). DOI: 10.17076/them1247

6. Skamnitskaya L.S., Bubnova T.P., Svetov S.A. Prospects of the use of Archean silicites of Central Karelia (Elmusskaya and Koykarskaya structures) for producing building materials. *Construction materials*. 2017. N 9, p. 62-66 (in Russian).

7. Svetov S.A. Magmatic systems of the ocean-continent transition zone in the Archaean of the eastern part of the Fennoscandian Shield. Petrozavodsk: Karel'skii nauchnyi tsentr RAN, 2005, p. 230 (in Russian).

8. Svetov S.A. Ancient adakites of the Fennoscandian Shield. Petrozavodsk: Karel'skii nauchnyi tsentr RAN, 2009, p. 115 (in Russian).

9. Skamnitskaya L.S., Bubnova T.P. Feldspathic Raw Materials of the Republic of Karelia: A Condition and Prospects. *Gornyi zhurnal*. 2015. N 5, p. 23-26 (in Russian).

10. Medvedev P.V., Svetov S.A., Svetova A.I. Relics of Thermophylic Chemolithotrophic Microbiota in the Archean Rocks from Central Karelia. *Karelian Research Centre of the RAS*. 2014. N 1, p. 135-147 (in Russian).

11. Svetov S.A., Medvedev P.V. Mesoarchean silicites, a unique environment for the preservation of early life. *Litosfera*. 2013. N 6, p. 3-13 (in Russian).

12. Metallogeny of Karelia. Ed. by S.I.Rybakov, A.I.Golubev. Petrozavodsk: Karel'skii nauchnyi tsentr RAN, 1999, p. 340 (in Russian).

13. Onega Paleoproterozoic structure (geology, tectonics, deep structure, and metallogeny). Petrozavodsk: Karel'skii nauchnyi tsentr RAN, 2011, p. 431 (in Russian).
14. Precambrian stratigraphy of Karelia. Reference sections of the Upper Archean deposits. Petrozavodsk: Karel'skii nauchnyi tsentr RAN, 1992, p. 190 (in Russian).
15. Yudovich Ya.E., Ketris M.P. Main regularities of manganese geochemistry. Syktyvkar: Komi nauchnyi tsentr Ural'skogo otdeleniya RAN, 2013, p. 40 (in Russian).
16. Rusakov V.Yu. Formation mechanisms of marine hydrothermal sedimentary deposits (exemplified by the Quaternary hydrothermal fields of the Mid-Atlantic Ridge and hydrothermal sedimentary Middle Paleozoic deposits of the Southern Urals: Avtoref. dis. … d-ra geol.-mineral. nauk. Moscow: Institut geokhimii i analiticheskoi khimii im. V.I.Vernadskogo, 2014, p. 55 (in Russian).
17. Yudovich Ya.E., Ketris M.P., Rybina N.V. Geochemistry of titanium. Syktyvkar: Geoprint, 2018, p. 432 (in Russian).
18. Yudovich Ya.E., Ketris M.P. Geochemical indicators of lithogenesis (lithological geochemistry). Syktyvkar: Geoprint, 2011, p. 732 (in Russian).
19. Gromet L.P., Dymek R.F., Haskin L.A., Korotev R.L. The "North American shale composite": Its compilations, major and trace element characteristics. *Geochimica et Cosmochimica Acta*. 1984. Vol. 48. Iss. 12, p. 2469-2482. DOI: 10.1016/0016-7037(84)90298-9
20. Sugitani K., Yamamoto K., Adachi M. et al. Archean cherts derived from chemical, biogenic and clastic sedimentation in a shallow restricted basin: examples from the Gorge Creek Group in the Pilbara Block. *Sedimentology*. 1998. Vol. 45. Iss. 6, p. 1045-1062. DOI: 10.1046/J.1365-3091.1998.00198.x
21. Sugitani K. Geochemical characteristics of Archean cherts and other sedimentary rocks in the Pilbara Block, Western Australia: evidence for Archean seawater enriched in hydrothermally-derived iron and silica. *Precambrian Research*. 1992. Vol. 57. Iss.1-2, p. 21-47. DOI: 10.1016/0301-9268(92)90093-4
22. Brengman L.A., Fedo C.M., Whitehouse M.J. Evaluating the geochemistry and paired silicon and oxygen isotope record of quartz in siliceous rocks from the ~3 Ga Buhwa Greenstone Belt, Zimbabwe, a critical link to deciphering the Mesoarchean silica cycle. *Chemical Geology*. 2021. Vol. 577. N 120300. DOI: 10.1016/j.chemgeo.2021.12030
23. Ledevin M. Archean Cherts: Formation Processes and Paleoenvironments. *Earth's Oldest Rocks. Second Edition*. Elsevier, 2019, p. 913-938.
24. Strekopytov S.V., Dubinin A.V., Volkov I.I. Behaviour of REE, zirconium, and hafnium in sediments and nodules of the Trans-Pacific line. *Geokhimiya*. 1995. N 7, p. 985-996 (in Russian).
25. Abraham K., Hofmann A., Foley S.F. et al. Coupled silicon-oxygen isotope fractionation traces Archaean silicification. *Earth and Planetary Science Letters*. 2011. Vol. 301. Iss. 1-2, p. 222-230. DOI: 10.1016/j.epsl.2010.11.002
26. Deutschmann C., Hopp J., Trieloff M., Ott U. Entrapment history of aqueous Ÿuids in Archean cherts from the Barberton Greenstone Belt, South Africa. *Precambrian Research*. 2022. Vol. 368. N 106502, p. 1-14. DOI: 10.1016/j.precamres.2021.106502
27. Boorn van den S.H.J.M., Bergen van M.J., Nijman W., Vroon P.Z. Dual role of seawater and hydrothermal fluids in Early Archean chert formation: Evidence from silicon isotopes. *Geology*. 2007. Vol. 35. N 10, p. 939-942. DOI: 10.1130/G24096A.1
28. Marin-Carbonne J., Chaussidon M., Robert F. Micrometer-scale chemical and isotopic criteria (O and Si) on the origin and history of Precambrian cherts: implications for paleo-temperature reconstructions. *Geochimica et Cosmochimica Acta*. 2012. Vol. 92, p. 129-147. DOI: 10.1016/j.GCA.2012.05.040
29. Rouchon V., Orberger B. Origin and mechanisms of K-Si-metasomatism of ca. 3.4-3.3 Ga volcaniclastic deposits and implications for Archean seawater evolution: Examples from cherts of Kittys Gap (Pilbara craton, Australia) and Msauli (Barberton Greenstone Belt, South Africa). *Precambrian Research*. 2008. Vol. 165. Iss. 3-4, p. 169-189. DOI: 10.1016/j.precamres.2008.06.003
30. Belousov V.I., Rychagov S.N., Sugrobov V.M. North Paramushir hydrothermal magmatic convective system: geological structure, conceptual model, geothermal resources. *Vulkanologiya i seismologiya*. 2002. N 1, p. 34-50 (in Russian).
31. Qiannan Hu, Xin Zhang, Fuqing Jiang et al. Geochemical characteristics of hydrothermal sediments from Iheya North Knoll in the Okinawa Trough. *Chinese Journal of Oceanology and Limnology*. 2017. Vol. 35, p. 947-955. DOI: 10.1007/s00343-017-6035-3
32. Xiaoyu Zhang, Chunhui Tao, Xuefa Shi et al. Geochemical characteristics of REY-rich pelagic sediments from the GC02 in central Indian Ocean Basin. *Journal of Rare Earths*. 2017. Vol. 35. Iss. 10, p. 1047-1058. DOI: 10.1016/S1002-0721(17)61012-3
33. Shili Liao, Chunhui Tao, Huaiming Li et al. Surface sediment geochemistry and hydrothermal activity indicators in the Dragon Horn area on the Southwest Indian Ridge. *Marine Geology*. 2018. Vol. 398, p. 22-34. DOI: 10.1016/j.margeo.2017.12.005
34. Ledevin M., Arndt N., Simionovici A. et al. Silica precipitation triggered by clastic sedimentation in the Archean: new petrographic evidence from cherts of the Kromberg type section, South Africa. *Precambrian Research*. 2014. Vol. 255. Part 1, p. 316-334. DOI: 10.1016/j.precamres.2014.10.009
35. Svetova E.N., Svetov S.A., Danilevskaya L.A. Rare and Rare Earth Elements in Quartz as Indicators of Minerogenesis. *Karelian Research Centre of the RAS*. 2012. N 3, p. 137-145 (in Russian).

***Authors*: Natalya I. Kondrashova,** *Candidate of Geological and Mineralogical Sciences, Researcher, Associate Professor, https://orcid.org/0000-0002-2323-231X* (*Institute of Geology, Karelian Research Centre of the RAS, Petrozavodsk, Russia*; *Petrozavodsk State University, Petrozavodsk, Russia*), **Tatyana P. Bubnova,** *Researcher, https://orcid.org/0000-0003-3513-8520* (*Institute of Geology, Karelian Research Centre of the RAS, Petrozavodsk, Russia*), **Pavel V. Medvedev,** *Candidate of Geological and Mineralogical Sciences, Senior Researcher, pmedved@krc.Karelia.ru, https://orcid.org/0000-0002-4098-5321* (*Institute of Geology, Karelian Research Centre of the RAS, Petrozavodsk, Russia*).

The authors declare no conflict of interests.